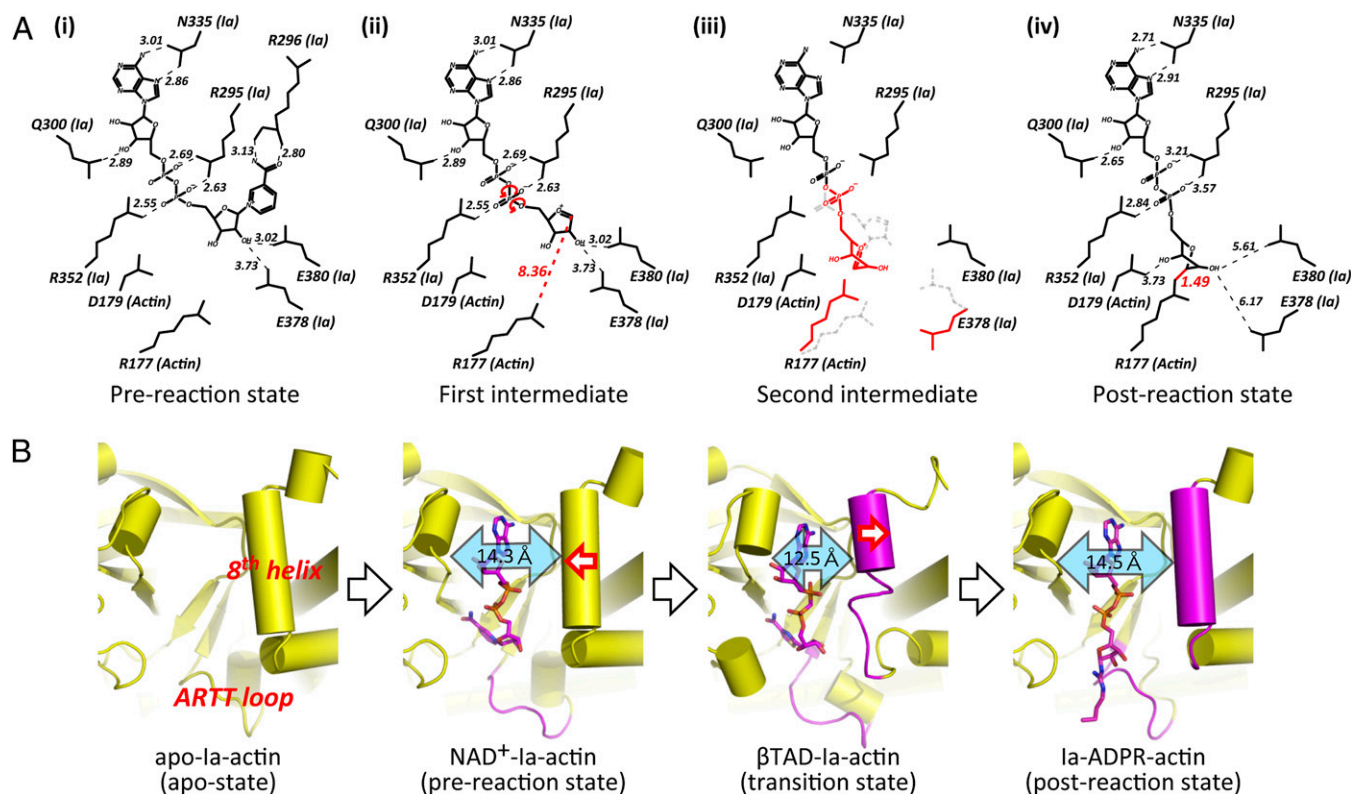


# Corrections

## BIOCHEMISTRY

Correction for “Arginine ADP-ribosylation mechanism based on structural snapshots of iota-toxin and actin complex,” by Toshiharu Tsurumura, Yayoi Tsumori, Hao Qiu, Masataka Oda, Jun Sakurai, Masahiro Nagahama, and Hideaki Tsuge, which appeared in issue 11, March 12, 2013, of *Proc Natl Acad Sci USA* (110:4267–4272; first published February 4, 2013; 10.1073/pnas.1217227110).

The authors note that Fig. 7 appeared incorrectly. There was a drawing error in the nicotinamide of NAD<sup>+</sup> within Fig. 7*A*, and distance values were refined based on the last coordinate. The corrected figure and its legend appear below. This error does not affect the conclusions of the article.



**Fig. 7.** Schematic illustrating the mechanism of ADP-ribosylation. (A) SN1 mechanism in Ia: (i) NAD<sup>+</sup>-Ia-Actin as the prereaction state; (ii) nicotinamide cleavage occurs via an SN1 reaction induced by an NMN ring-like structure and the first oxocarbenium cation intermediate is formed with a strained conformation; (iii) the second cationic intermediate is induced through alleviation of the strained conformation mainly by O3-NP and NP-NO5 rotation, and then NC1 of N-ribose nucleophilically attacks Arg177 of actin; (iv) Ia-ADPR-actin as the postreaction state. (B) Successive structures during ADP-ribosylation and the structure of each reaction: step 1 [apo-Ia-actin (apo-state)], step 2 [NAD<sup>+</sup>-Ia-actin (pre-reaction state)], step 3 [βTAD-Ia-actin (transition state)], and step 4 [Ia-ADPR-actin (post-reaction state)].

www.pnas.org/cgi/doi/10.1073/pnas.1304997110

## ENVIRONMENTAL SCIENCES

Correction for “Cesium-137 deposition and contamination of Japanese soils due to the Fukushima nuclear accident,” by Teppei J. Yasunari, Andreas Stohl, Ryugo S. Hayano, John F. Burkhart, Sabine Eckhardt, and Tetsuzo Yasunari, which appeared in issue 49, December 6, 2011, of *Proc Natl Acad Sci USA* (108:19530–19534; first published November 14, 2011; 10.1073/pnas.1112058108).

The authors note the following: “Due to the corrections on some of the observed daily  $^{137}\text{Cs}$  deposition numbers made by the MEXT (Ministry of Education, Culture, Sports, Science and Technology in Japan; available on the MEXT website in Japanese at <http://radioactivity.mext.go.jp/ja/list/195/list-1.html>) mainly at Kanagawa prefecture along with some minor corrections at other prefectures, the objectively estimated deposition values in the paper have been revised by using the updated input data on the observed  $^{137}\text{Cs}$  deposition by MEXT.”

The authors also note that on page 19530, left column, within the abstract, lines 22–23, “were estimated to be more than 5.6 and 1.0 PBq, respectively” should instead appear as “were estimated to be approximately 6.7 and 1.3 PBq, respectively.”

On page 19531, left column, second full paragraph, line 5, “(TRMM, 3B42 V6 product)” omitted the following references:

27. Huffman GJ (1997) Estimates of root-mean-square random error for finite samples of estimated precipitation. *J Appl Meteor* 36:1191–1201.
28. Huffman GJ, et al. (2007) The TRMM multisatellite precipitation analysis (TMPA): Quasi-global, multiyear, combined-sensor precipitation estimates at fine scales. *J Hydrometeorol* 8(1):38–55.

On page 19531, right column, first full paragraph, lines 4–8, “Our estimates show that the area around NPP in Fukushima, secondarily effected areas (Miyagi and Ibaraki prefectures), and other effected areas (Iwate, Yamagata, Tochigi, and Chiba prefectures) had  $^{137}\text{Cs}$  depositions of more than 100,000, 25,000, and 10,000 MBq  $\text{km}^{-2}$ , respectively” should instead appear as “Our estimate in Fig. 24 for the case of DRT of 0.005 showed that the area around the Nuclear Power Plant (NPP) in Fukushima, secondarily effected areas (Miyagi prefecture), and other effected areas (Iwate, Yamagata, Tochigi, Ibaraki, and Chiba prefectures) had partially  $^{137}\text{Cs}$  depositions of more than 100,000, 50,000, and 10,000 MBq  $\text{km}^{-2}$ , respectively.”

On page 19531, right column, first full paragraph, lines 22–23, “on the similar order of the MEXT/DOE observations using a DRT value of 0.001 (Fig. S4)” should instead appear as “closer to the order of the MEXT/DOE observations around the NPP using a DRT value of 0.001 (Fig. S4).”

On page 19533, left column, first paragraph, lines 1–6, “some neighboring prefectures such as Miyagi, Tochigi, and Ibaraki are partially close to the limit under our upper bound estimate (Movie

S4) and, therefore, local-scale exceedance is likely given the strong spatial variability of  $^{137}\text{Cs}$  deposition. For those three prefectures, detailed soil sampling is recommended in the near future” should instead appear as “some neighboring prefectures such as Iwate, Yamagata, Miyagi, Tochigi, and Ibaraki are partially close to the limit under the upper bound estimate with DRT of 0.001 (i.e., “the highest deposition estimate” in our estimates with DRTs of 0.001–0.1) [using CCs of 38, 53, and 68  $\text{kg m}^{-2}$  (Movie S4)] and, therefore, local-scale exceedance is likely given the strong spatial variability of  $^{137}\text{Cs}$  deposition. For those prefectures, detailed soil sampling is recommended in the near future.”

On page 19533, left column, second full paragraph, line 1, “We estimate that a total of more than 5.6 and 1.0 PBq  $^{137}\text{Cs}$ ” should instead appear as “We estimate that a total of approximately 6.7 and 1.3 PBq  $^{137}\text{Cs}$ .”

On page 19533, left column, second full paragraph, line 9, “(Fig. 3)” should instead appear as “with DRT of 0.001 using CC of 53  $\text{kg m}^{-2}$  (Fig. 3).”

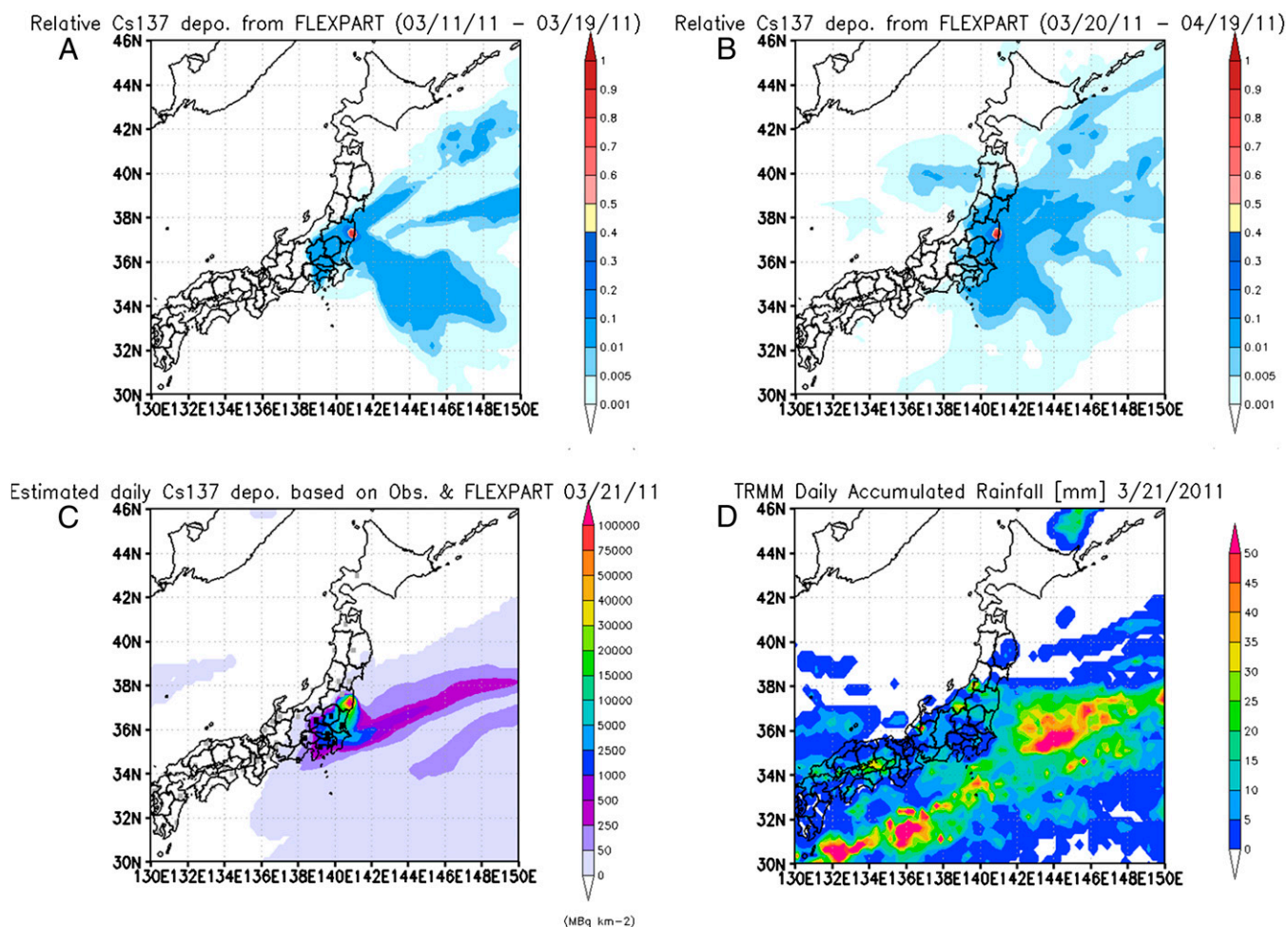
On page 19533, left column, second full paragraph, lines 13–15, “such as Iwate, Miyagi, Yamagata, Niigata, Tochigi, Ibaraki, and Chiba, where values of more than 250 Bq  $\text{kg}^{-1}$  cannot be excluded (Fig. 3 and Movie S4)” should instead appear as “such as Iwate, Miyagi, Yamagata, Niigata, Tochigi, Ibaraki, Chiba, etc., where values of more than 250 Bq  $\text{kg}^{-1}$  cannot be excluded for the estimated soil contaminations under the upper bound estimate on the deposition with DRT of 0.001 (i.e., “the highest deposition estimate” in our estimates with DRTs of 0.001–0.1) using CCs of 38, 53, and 68  $\text{kg m}^{-2}$  (Fig. 3 and Movie S4).”

On page 19533, left column, second full paragraph, line 20 before “Therefore,” the following sentence should be added: “In addition, the spatiotemporally limited  $^{137}\text{Cs}$  deposition data by the MEXT observations were used in our estimates, which also included such as no measurements (Miyagi) and missing observations (Yamagata and Fukushima) for the time period in this study.”

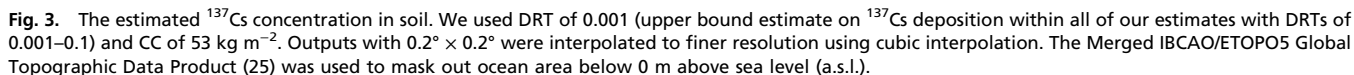
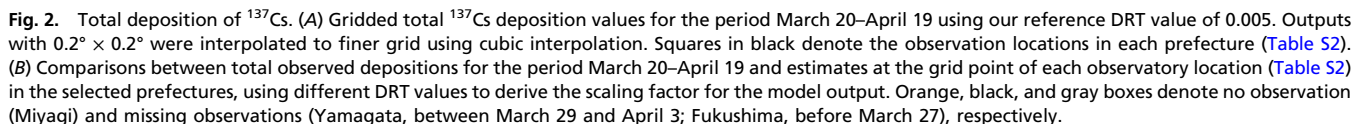
On page 19533, right column, first paragraph, lines 3–4, “Fukushima, March 18–March 26 and April 4; Gifu, March 24, 25, 27, 28, and 30; Nara, March 18–21 and April 15–18” should instead appear as “Fukushima, March 18–March 26; Gifu, March 24; Nara, March 18–20 and April 15–18.”

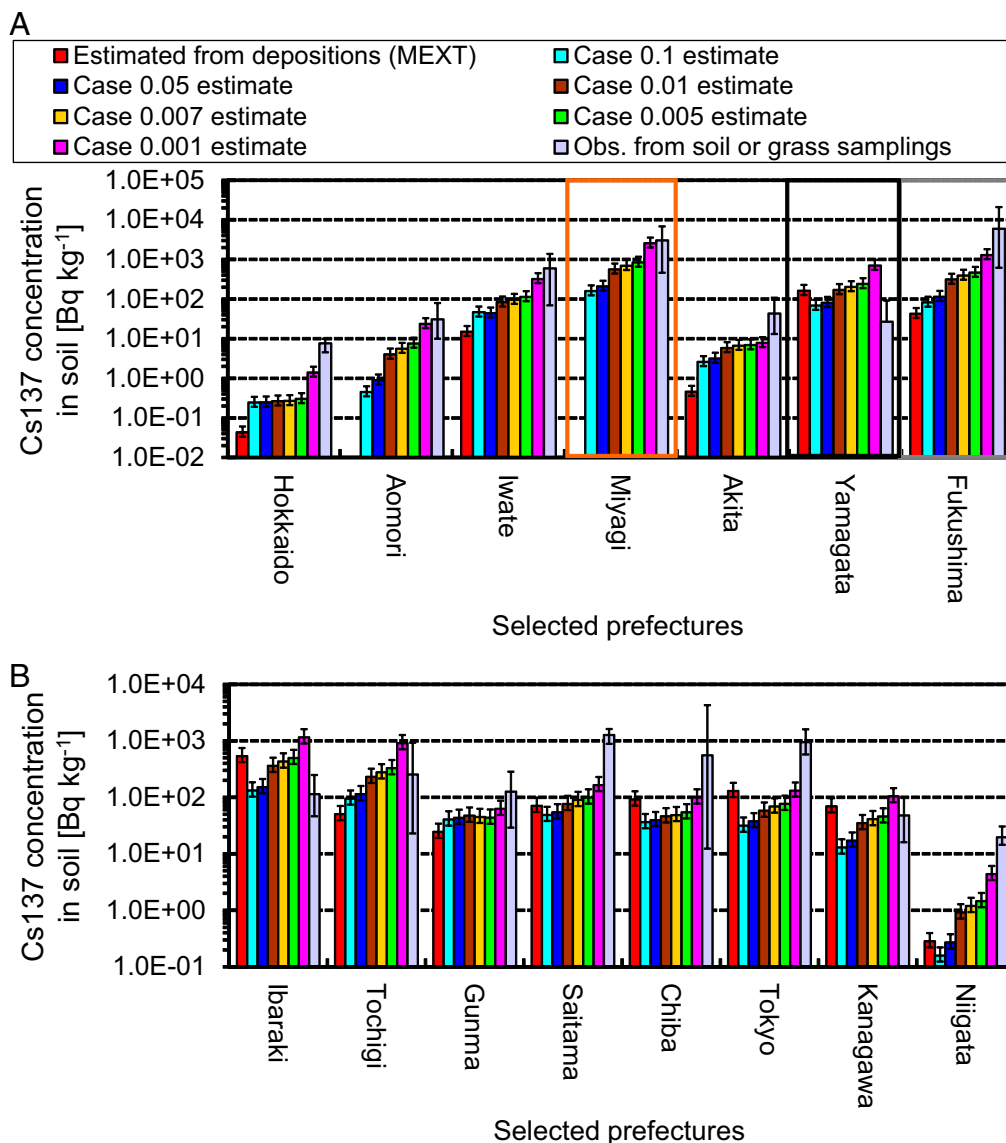
On page 19533, right column, second full paragraph, line 18, “counting  $N$  on each day” should instead appear as “counting  $N$  on each day, for which unavailable, missing, and no detection on the observed depositions were all computationally treated as zero deposition.”

Last, the legends for Figs. 1, 2, 3, and 4 appeared incorrectly. The figures and their corrected legends appear below. These errors do not affect the conclusions of the article.



**Fig. 1.** Cesium-137 deposition maps. (A) Relative deposition contributions between March 11 and 19, showing the areas potentially effected by  $^{137}\text{Cs}$  before the start of measurements. The sums of the depositions during the period were divided by the maximum deposition in the accumulated field. (B) The same as in A, but for March 20–April 19. (C) An example of estimated daily deposition of  $^{137}\text{Cs}$  on March 21. Squares in gray and black denote observatories (Table S2) that did have computational zero  $^{137}\text{Cs}$  deposition (unavailable, missing, or no detection) or daily DR = 0, and detected the depositions used for making the estimation map for the deposition, respectively. (D) Daily accumulated rainfall on March 21 by TRMM [3B42 V6 product: (27, 28)].







# Cesium-137 deposition and contamination of Japanese soils due to the Fukushima nuclear accident

Teppei J. Yasunari<sup>a,1</sup>, Andreas Stohl<sup>b</sup>, Ryugo S. Hayano<sup>c</sup>, John F. Burkhart<sup>b,d</sup>, Sabine Eckhardt<sup>b</sup>, and Tetsuzo Yasunari<sup>e</sup>

<sup>a</sup>Universities Space Research Association, Goddard Earth Sciences Technology and Research, Columbia, MD 21044; <sup>b</sup>Norwegian Institute for Air Research, P.O. Box 100, N-2027 Kjeller, Norway; <sup>c</sup>Department of Physics, University of Tokyo, 7-3-1 Hongo, Bunkyo-ku, Tokyo 113-0033, Japan; <sup>d</sup>Sierra Nevada Research Institute, University of California, Merced, 5200 North Lake Road, Merced, CA 95343; and <sup>e</sup>Hydrospheric Atmospheric Research Center, Nagoya University, Nagoya, Aichi 464-8601, Japan

Edited by James E. Hansen, Goddard Institute for Space Studies, New York, NY, and approved October 5, 2011 (received for review July 25, 2011)

The largest concern on the cesium-137 ( $^{137}\text{Cs}$ ) deposition and its soil contamination due to the emission from the Fukushima Daiichi Nuclear Power Plant (NPP) showed up after a massive quake on March 11, 2011. Cesium-137 ( $^{137}\text{Cs}$ ) with a half-life of 30.1 y causes the largest concerns because of its deleterious effect on agriculture and stock farming, and, thus, human life for decades. Removal of  $^{137}\text{Cs}$  contaminated soils or land use limitations in areas where removal is not possible is, therefore, an urgent issue. A challenge lies in the fact that estimates of  $^{137}\text{Cs}$  emissions from the Fukushima NPP are extremely uncertain, therefore, the distribution of  $^{137}\text{Cs}$  in the environment is poorly constrained. Here, we estimate total  $^{137}\text{Cs}$  deposition by integrating daily observations of  $^{137}\text{Cs}$  deposition in each prefecture in Japan with relative deposition distribution patterns from a Lagrangian particle dispersion model, FLEXPART. We show that  $^{137}\text{Cs}$  strongly contaminated the soils in large areas of eastern and northeastern Japan, whereas western Japan was sheltered by mountain ranges. The soils around Fukushima NPP and neighboring prefectures have been extensively contaminated with depositions of more than 100,000 and 10,000 MBq  $\text{km}^{-2}$ , respectively. Total  $^{137}\text{Cs}$  depositions over two domains: (i) the Japan Islands and the surrounding ocean (130–150°E and 30–46°N) and, (ii) the Japan Islands, were estimated to be more than 5.6 and 1.0 PBq, respectively. We hope our  $^{137}\text{Cs}$  deposition maps will help to coordinate decontamination efforts and plan regulatory measures in Japan.

aerosol | dispersion modeling | radioactive fallout

A catastrophic earthquake and tsunami occurred on March 11, 2011, which caused destruction in northeastern Japan and severely damaged the Fukushima Daiichi Nuclear Power Plant (NPP). This event led to emissions of radioactive materials from the NPP (1), albeit at unknown and likely strongly varying release rates (1–3). Among these materials, with a half-life of 30.1 y (4), cesium-137 ( $^{137}\text{Cs}$ ) causes the largest concerns because of its deleterious effect on agriculture and stock farming, and, thus, human life for decades. Removal of  $^{137}\text{Cs}$ -contaminated soils or land use limitations in areas where removal is not possible is, therefore, an urgent issue. The Japanese government, general public, and scientists have been waiting for the information of the spatial distributions of  $^{137}\text{Cs}$  deposition and its soil contamination over all of Japan.

The aerosol-bound  $^{137}\text{Cs}$  can be removed from the atmosphere and brought to the surface by dry or wet deposition. Analysis of data collected after the Chernobyl accident has shown that  $^{137}\text{Cs}$  adsorbed in the top soil layer can remain there for many years (5, 6), restricting land use, e.g., for food production, of highly contaminated areas for a long time. To minimize the impacts on human health of soil contamination in Japan due to the Fukushima NPP accident, spatial maps of  $^{137}\text{Cs}$  deposition and concentrations in soil are urgently needed. Sporadic sampling of the soils in and around Fukushima prefecture has been carried out after the NPP accident under the instruction by the Ministry of Education, Culture, Sports, Science and Technology (MEXT)

(7) and others (Table S1). However, it is impossible to fully capture the distribution of  $^{137}\text{Cs}$  deposition across Japan from a limited number of in situ measurements alone. On the other hand, reliable estimates using dispersion models are also not available because of the largely unknown source term. Not only is the total release of  $^{137}\text{Cs}$  from the damaged NPP poorly known, but also its variation with time is even more uncertain. Although first attempts to estimate it have been made (2) and another study tried to estimate its deposition based on the previous study (2) over the limited areas around Fukushima prefecture with a regional chemical transport model (8), these estimates on the emission rate are highly uncertain and the discussion on deposition over all of Japan has not been made.

In this study we quantitatively estimate the spatial distribution of the  $^{137}\text{Cs}$  deposition and its soil contamination over all of Japan. We take relative deposition distribution patterns from a Lagrangian particle dispersion model, FLEXPART (*Materials and Methods* and *SI Text*) (9), using a constant source term [as assumed also in some simulations because of high uncertainty of the emission amount (10–16)]. We fuse daily varying observations of  $^{137}\text{Cs}$  deposition in each Japanese prefecture (17) into the modeled deposition fields to obtain quantitative deposition estimates.

## Results

Our estimate of  $^{137}\text{Cs}$  deposition is made for the period between March 20 and April 19 because no observations of  $^{137}\text{Cs}$  deposition were made between March 12 and 17 and the dispersion model did not simulate any depositions at the observation locations on March 18 and 19 (Fig. S1). Thus, our quantitative estimates do not include the first 8 d after the NPP accident, yet for that period we provide relative contributions to the deposition. In Fig. 1A we show the relative contribution map of the deposition over the period when our estimate was not applicable. It shows that before March 20, potentially contaminated air masses were mainly transported toward the Pacific Ocean and  $^{137}\text{Cs}$  deposition would have occurred mostly over the ocean, except for Fukushima prefecture and some neighboring provinces. Between March 20 and April 19 (Fig. 1B), a much wider area was effected by the deposition. In particular, eastern and northeastern parts of Japan had a greater potential for  $^{137}\text{Cs}$  deposition, whereas in western Japan the potential for  $^{137}\text{Cs}$  deposition was low. Overall, however, the highest potential deposition occurred over the Pacific Ocean, where a few observations of  $^{137}\text{Cs}$  deposition exist

Author contributions: T.J.Y. designed research; T.J.Y., A.S., J.F.B., and S.E. performed research; T.J.Y. and R.S.H. analyzed data; and T.J.Y., A.S., J.F.B., and T.Y. wrote the paper.

The authors declare no conflict of interest.

This article is a PNAS Direct Submission.

Freely available online through the PNAS open access option.

See Commentary on page 19447.

<sup>1</sup>To whom correspondence should be addressed: E-mail: tyasunari@usra.edu.

This article contains supporting information online at [www.pnas.org/lookup/suppl/doi:10.1073/pnas.1112058108/-DCSupplemental](http://www.pnas.org/lookup/suppl/doi:10.1073/pnas.1112058108/-DCSupplemental).

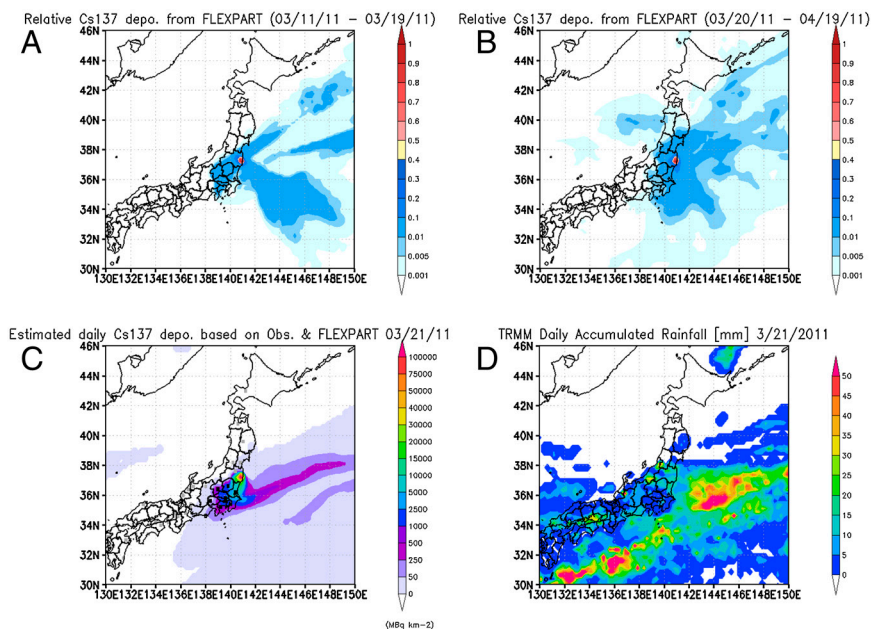


**Fig. 1.** Cesium-137 deposition maps. (A) Relative deposition contributions between March 11 and 19, showing the areas potentially effected by  $^{137}\text{Cs}$  before the start of measurements. The sums of the depositions during the period were divided by the maximum deposition in the accumulated field. (B) The same as in A, but for March 20–April 19. (C) An example of estimated daily deposition of  $^{137}\text{Cs}$  on March 21. Squares in black denote the observation locations in each prefecture (Table S2). (D) Daily accumulated rainfall on March 21 by TRMM.

(18), showing that winds were generally quite favorable and carried most radiation away from populated areas.

From March 20, we can estimate  $^{137}\text{Cs}$  deposition fields over Japan more reliably because daily observations have been made in most Japanese prefectures (17) (Table S2). For days from March 20, we create deposition estimates using scaled model values [hereafter called, deposition ratio (DR); see *Materials and Methods*] from a constant source term simulation in conjunction with the measurements from the MEXT observation network (17). An example of a three-hourly DR animation map is available in Movie S1. For periods when the simulated daily DR value is close to zero yet deposition is observed, a threshold factor is employed in Eq. 2 (*Materials and Methods* and *SI Text*). In such cases, a minimum positive deposition ratio value, hereafter called DR threshold (DRT), needs to be used to derive the scaling (*Materials and Methods* and *SI Text*). The choice of this DRT is subjective and also effects the estimated deposition amount in our method. After performing comparisons with the observed depositions in each prefecture (*SI Text*, Fig. S2, and Table S3), we used a DRT of 0.005 for the best guess estimate of daily deposition between March 20 and April 19 (Movie S2) but we also report derived deposition estimates for other DRT values.

The simulated distribution of  $^{137}\text{Cs}$  deposition is closely linked to precipitation as shown for the case of March 21 (Fig. 1 C and D). The highest deposition values downwind of the NPP are clearly aligned with satellite-observed precipitation by tropical rainfall measuring mission (TRMM, 3B42 V6 product) in a frontal rain band, which causes washout of the radionuclides (Movie S2 and S3). Comparison of daily observed precipitation fields with the estimated deposition maps shows that  $^{137}\text{Cs}$  deposition is simulated mainly when frontal rain bands pass over Japan (Movie S2). It was reported previously (19) that around 90% of the total deposition of  $^{137}\text{Cs}$  occurs with precipitation. Thus, the general agreement between observed precipitation and simulated deposition confirms that the model captures the main deposition events, which is also consistent with the discussion from the study by using a regional chemical transport model (8). The daily  $^{137}\text{Cs}$  deposition was frequently detected at observatories (17) in the eastern and northeastern prefectures of Japan from March 20. Furthermore, large increases of atmospheric

radioactivity in the prefectures around Fukushima were observed (20) on March 22 (Fig. S3), probably reflecting ground shine radiation from the radionuclides deposited during the rainfall event on March 21 (Fig. 1 C and D).

Maps of the total  $^{137}\text{Cs}$  deposition between March 20 and April 19 are shown in Fig. 2A. As a general characteristic, most of the eastern parts of Japan were effected by a total  $^{137}\text{Cs}$  deposition of more than  $1,000 \text{ MBq km}^{-2}$ . Our estimates show that the area around NPP in Fukushima, secondarily effected areas (Miyagi and Ibaraki prefectures), and other effected areas (Iwate, Yamagata, Tochigi, and Chiba prefectures) had  $^{137}\text{Cs}$  depositions of more than  $100,000$ ,  $25,000$ , and  $10,000 \text{ MBq km}^{-2}$ , respectively. Airborne and ground-based survey measurements jointly carried out by MEXT and the US Department of Energy (DOE) (21) show high  $^{137}\text{Cs}$  deposition amounts were observed northwestward and up to a distance of 80 km from Fukushima NPP. It was estimated from the first measurement that by April 29, more than  $600,000 \text{ MBq km}^{-2}$  had been deposited in the area, which is greater than our estimate of less than  $500,000 \text{ MBq km}^{-2}$  (Fig. 2A), yet well within the range of uncertainty of our method (Fig. S4). Furthermore, because no observations on daily deposition were available before March 27 in Fukushima City (Fig. 2B) and no daily deposition observations around NPP, our estimates are expected to underestimate the total deposition in the vicinity of the NPP. In conducting sensitivity studies with DRT, our estimates provide values on the similar order of the MEXT/DOE observations using a DRT value of 0.001 (Fig. S4).

Using an approximate relationship between  $^{137}\text{Cs}$  deposition and its topsoil concentration (22) [conversion coefficient (CC) of  $53 \pm 15 \text{ kg m}^{-2}$ ] (Fig. S5), we converted the estimated depositions into topsoil concentrations (Fig. 3, Movie S4, and Table S4).

We compared  $^{137}\text{Cs}$  concentrations in the topsoil derived from both observed  $^{137}\text{Cs}$  deposition values (17) and from our estimates, with direct measurements of  $^{137}\text{Cs}$  concentrations in soils and grasses with a soil-to-grass transfer factor of 0.13 (23) (*SI Text* and Table S1) (Fig. 4). The MEXT deposition-based soil contamination tends to be lower than the soil- and grass-based samplings because of the latter including the time period just after the NPP accident. Our scaled model deposition fields agree well with both the point measurements including the MEXT areal surveys and

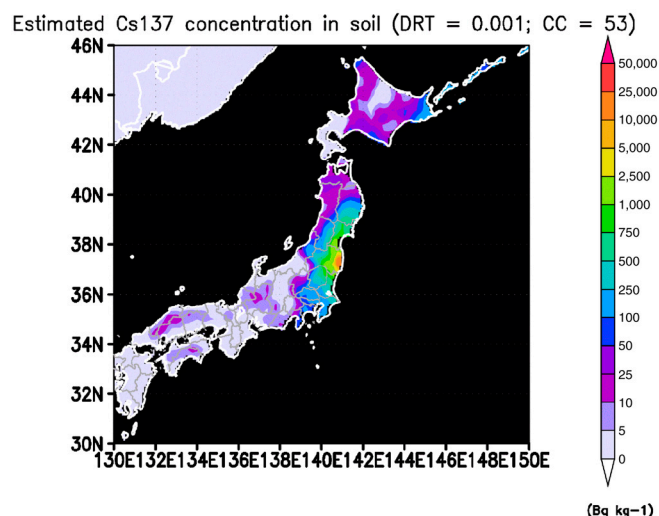


**Fig. 2.** Total deposition of  $^{137}\text{Cs}$ . (A) Gridded total  $^{137}\text{Cs}$  deposition values for the period March 20–April 19 using our reference DRT value of 0.005. Outputs with  $0.2^\circ \times 0.2^\circ$  were interpolated to finer grid using cubic interpolation. Squares in black denote the observation locations in each prefecture (Table S2). (B) Comparisons between total observed depositions for the period March 20–April 19 and estimates at the grid point of each observatory location (Table S2) in the selected prefectures, using different DRT values to derive the scaling factor for the model output. Orange, gray, and black boxes denote no observation (Miyagi) and missing observations (Yamagata, between March 29 and April 3; Fukushima, before March 27 and April 4), respectively.

**A**

Estimated from depositions (MEXT)

- Case 0.1 estimate
- Case 0.05 estimate
- Case 0.007 estimate
- Case 0.001 estimate
- Case 0.01 estimate
- Case 0.005 estimate
- Obs. from soil or grass samplings

Cs137 concentration in soil [Bq kg<sup>-1</sup>]

Selected prefectures

**B**

Cs137 concentration in soil [Bq kg<sup>-1</sup>]

Selected prefectures

**Fig. 4.** Atmospheric, soil, and grass observation-based Cs-137 concentrations, and estimates based on the scaled model output and for different DRT values used for the scaling. (A) Comparisons in northern prefectures. Aomori and Miyagi prefectures had no  $^{137}\text{Cs}$  detections on the daily deposition data and no measurements, respectively. The minimum value in Yamagata prefecture is no detection and no lower error bar is shown. (B) The same as in A, but around Kanto area. Lower and upper error bars denote minimum and maximum concentrations using CC of 68 and  $38 \text{ kg m}^{-2}$  based on Fig. S5, respectively. Orange, gray, and black boxes denote no observation (Miyagi) and missing observations (Yamagata, between March 29 and April 3; Fukushima, before March 27 and April 4), respectively. A soil-to-grass transfer factor of 0.13 (23) was used to convert grass to soil contamination. For Fukushima prefecture, only the soil observations in Fukushima City were used, excluding other observations close to the Fukushima NPP. The data source for the comparisons are summarized in Table S1.



Fukushima prefecture exceeded this limit and some neighboring prefectures such as Miyagi, Tochigi, and Ibaraki are partially close to the limit under our upper bound estimate (Movie S4) and, therefore, local-scale exceedance is likely given the strong spatial variability of  $^{137}\text{Cs}$  deposition. For those three prefectures, detailed soil sampling is recommended in the near future. Estimated and observed contaminations in the western parts of Japan were not as serious, even though some prefectures were likely effected to some extent (Fig. 3, Movie S4, and Table S4). Concentrations in these areas are below  $25 \text{ Bq kg}^{-1}$ , which is far below the threshold for farming. However, we strongly recommend each prefecture to quickly carry out some supplementary soil samplings at city levels to validate our estimates even if the concentrations are low.

The relatively low contamination levels over western Japan can be well explained by the Japanese topography. The eastern and northeastern parts of Japan are surrounded by mountain ranges such as the Kanto, Echigo, and Ohwu mountain ranges (Fig. S6) (25), which, to a large extent, sheltered the northwestern and western parts of Japan from the dispersion of radioactive material. It is worth noting, however, that relatively higher contamination levels can be seen over the Hida, Chugoku, and Shikoku mountain ranges (Fig. 3, Fig. S6, and Movie S4), probably due to orographic enhancement of precipitation and, thus, wet deposition of  $^{137}\text{Cs}$ . In Hokkaido, to the north of Japan's main island, both lower altitude and higher altitudes such as the Yubari and Hidaka mountain ranges are effected by  $^{137}\text{Cs}$  deposition, partially due to direct transport from the Fukushima NPP via the Pacific Ocean as shown in Movies S1 and S2 and also as simulated by another atmospheric transport model (12).

We estimate that a total of more than 5.6 and 1.0 PBq  $^{137}\text{Cs}$  were deposited over Japan and the surrounding ocean ( $130^{\circ}\text{--}150^{\circ}\text{E}$  and  $30^{\circ}\text{--}46^{\circ}\text{N}$ ), and the Japan Islands in this domain only, respectively (Fig. 24). Although the estimate for the larger domain is quite uncertain because it is constrained only by measurements in Japan, these numbers are consistent with a suspected total release of about 12 PBq  $^{137}\text{Cs}$  (2). Most of the deposition occurred over the Pacific Ocean, yet soil concentrations of  $^{137}\text{Cs}$  are above  $100 \text{ Bq kg}^{-1}$  over large areas of eastern Japan (Fig. 3). According to our results, food production in eastern Fukushima prefecture is likely severely impaired by the  $^{137}\text{Cs}$  loads of more than  $2,500 \text{ Bq kg}^{-1}$  (upper limit of farming) and also partially impacted in neighboring provinces such as Iwate, Miyagi, Yamagata, Niigata, Tochigi, Ibaraki, and Chiba, where values of more than  $250 \text{ Bq kg}^{-1}$  cannot be excluded (Fig. 3 and Movie S4). Notice also that our estimates are based on a transport model driven with meteorological analysis data from a global model. Such a model cannot fully capture all complexities of the regional wind field over Japan and, in particular, does not resolve the high spatiotemporal variability of precipitation. Therefore, we expect the true soil contamination across Japan to be considerably more variable than in our estimate. Even in regions where we find relatively low soil contamination levels, hot spots with high concentrations (e.g., due to convective rain fall, orographic enhancement of rainfall, or fine-grain soil flow by rainwater on the ground) may be possible. In contrast, relatively clean patches may also be present in areas with high overall contamination levels. Despite these shortcomings, we expect our results to be useful for regulatory measures and for guiding monitoring activities toward areas with expected high  $^{137}\text{Cs}$  burdens. We hope this study will contribute to understanding the contamination issue in Japan.

## Materials and Methods

**Observations of Cesium-137 Deposition and Concentration in Soil in each Prefecture.** From March 18, MEXT has been observing daily radioactivity levels in deposition in most of the prefecture (17). The exact coordinates of the sampling locations were individually accessible through our contacts to MEXT (Table S2). The deposition data between March 18 and 19 were not used in our estimate because of no depositions at observatories from the modeled

DR maps as mentioned in the main text. In some prefectures, data were missing or unavailable [Miyagi, March 18–April 19 (completely no observations); Yamagata, March 29–April 3; Fukushima, March 18–March 26 and April 4; Gifu, March 24, 25, 27, 28, and 30; Nara, March 18–21 and April 15–18; Oita, March 22–26].

**FLEXPART and Estimated  $^{137}\text{Cs}$  Deposition.** FLEXPART (9) is a Lagrangian particle dispersion model simulating transport, diffusion, dry and wet deposition, and radioactive decay of radioactive materials such as  $^{131}\text{I}$ ,  $^{137}\text{Cs}$ , and  $^{133}\text{Xe}$  (See <http://transport.nilu.no> for further details on FLEXPART). In this study, continuous emission from the Fukushima Daiichi NPP was assumed after 1800 hours coordinated universal time (UTC) on March 11, 2011. The simulation ended at 0000 hours UTC on April 20. FLEXPART was forced with the European Center for Medium-Range Weather Forecasts (ECMWF) operational analysis data with a global resolution of  $1^{\circ} \times 1^{\circ}$  and  $0.18^{\circ} \times 0.18^{\circ}$  for  $120^{\circ}\text{--}168^{\circ}\text{E}$  and  $25^{\circ}\text{--}50^{\circ}\text{N}$ . The output had a resolution of  $0.2^{\circ} \times 0.2^{\circ}$  and was recorded every 3 h (SI Text).

For each day, we first normalized the modeled daily accumulated deposition in each grid cell with the maximum accumulated deposition value for the model domain, hereafter called daily deposition ratio (DDR) maps:

$$DDR_{(x,y)} = \frac{1}{FPD_{\max i}} \sum_{i=1}^T FPD_{(x,y)i}, \quad [1]$$

where  $FPD_{(x,y)i}$  is the three-hourly modeled deposition in grid cell  $(x,y)$  and  $FPD_{\max}$  is the maximum daily deposition value found in the entire model domain.  $T$  is the number of model output timesteps per day ( $T = 8$ ). Daily gridded deposition values of  $^{137}\text{Cs}$  were estimated by scaling the DDR map with available daily observed  $^{137}\text{Cs}$  depositions in each prefecture by MEXT (17) by the following equation:

$$Depo_{(x,y)} = \frac{DDR_{(x,y)}}{N} \sum_{i=1}^N \frac{Depo_{i(Obs.)}}{DDR_{i(Obs.Loc.)}}, \quad [2]$$

where  $Depo_{(x,y)}$  is the estimated daily total  $^{137}\text{Cs}$  deposition in grid cell  $(x,y)$ ,  $Depo_{i(Obs.)}$  is the observed  $^{137}\text{Cs}$  deposition at location  $i$  (Table S2),  $N \leq 47$  is the number of available counts on a certain day in Japan's 47 prefectures,  $DDR_{i(Obs.Loc.)}$  is the  $DDR_{(x,y)}$  in the grid point where  $^{137}\text{Cs}$  deposition was observed, and  $DDR_{(x,y)}$  is the DDR in grid cell  $(x,y)$ . Only the cases with both the observed deposition and the  $DDR_{i(Obs.Loc.)}$  not equal to zero at each observatory location were used for counting  $N$  on each day. Because the  $Depo_{i(Obs.)}$  to  $DDR_{i(Obs.Loc.)}$  scaling factor in Eq. 2 becomes infinite when the simulated DDR value is close to zero but deposition is actually observed, a minimum positive DDR value, DRT, needs to be used to derive the scaling. Several DRTs of 0.001, 0.005, 0.007, 0.01, 0.05, and 0.1 for  $DDR_{i(Obs.Loc.)}$  within the simulation domain on each day were used to avoid abnormally high  $Depo_{(x,y)}$  values due to dividing by small values (SI Text). If  $DDR_{i(Obs.Loc.)}$  at a certain grid point was less than a DRT value,  $DDR_{i(Obs.Loc.)}$  was set to the DRT value.

For computing total  $^{137}\text{Cs}$  deposition between March 20 and April 19, we corrected all values to April 19 using a half-life of  $^{137}\text{Cs}$  of 30.1 y (4). The sum of all the daily observed or estimated  $^{137}\text{Cs}$  depositions is the total  $^{137}\text{Cs}$  deposition (Fig. 2 and Fig. S4A).

**Observations on  $^{137}\text{Cs}$  Concentrations in Soil and Grass.** For comparison with our estimates, measurements of  $^{137}\text{Cs}$  concentrations in soil or grass were used (SI Text and Table S1). Mean transfer factor of soil-to-grass of 0.13, which was obtained from the observations in Japanese soil and grass, was used to convert grass contamination to soil equivalent contamination (grass contamination divided by the transfer factor) (23). The times and locations of those samplings varied. To cover the time period of our study (March 20–April 19), we also used some soil samples from later dates, but we did not use any data after May 19. Notice also that the soil samples were also effected by  $^{137}\text{Cs}$  deposition before March 20 (SI Text). Some observatories measured total cesium concentration including both  $^{137}\text{Cs}$  and  $^{134}\text{Cs}$ . In that case, we assumed that half of the total Cs was  $^{137}\text{Cs}$ .

To convert the  $^{137}\text{Cs}$  deposition into soil concentration, soil depth and density information are needed. However, it is currently difficult to obtain this information across all of Japan. There is an empirical relationship on the ratio between  $^{137}\text{Cs}$  concentration and deposition from 0 to 5 cm soil, paddy soil, and field soil samples (22) (Fig. S5). We considered the mean value of the ratio as  $CC$  of  $53 \pm 15 \text{ kg m}^{-2}$  reflecting the 5-cm depth soil information and its density. Our estimated  $CC$  value is close to the  $CC$  value of  $65 \text{ kg m}^{-2}$  assumed by MEXT (26) with 5-cm soil and a soil density of

1,300 kg m<sup>-3</sup>.

Dividing our estimated deposition (MBq km<sup>-2</sup> = Bq m<sup>-2</sup>) by the CCs, we empirically obtained the mean <sup>137</sup>Cs concentration in soil (Bq kg<sup>-1</sup>).

**ACKNOWLEDGMENTS.** Useful comments were obtained from K.-M. Kim Morgan State University (MSU)/Goddard Earth Sciences Technology and Research (GESTAR) and Q. Tan Universities Space Research Association (USRA)/GESTAR. Daily deposition of radioactive materials, atmospheric radiations, and concentrations in soil used in this study were observed by the Ministry of Education, Culture, Sports, Science, and Technology (MEXT),

each prefecture in Japan, the Ministry of Agriculture, Forestry and Fisheries (MAFF), and Prof. Yamazaki et al. at Kinki University. We also appreciate all the people working on these measurements. The tropical rainfall measuring mission (TRMM, 3B42 V6 product) data used in this study were acquired using the Goddard Earth Sciences (GES)-Data and Information Services Center (DISC) as part of the National Aeronautics and Space Administration's GES-DISC. The Grid Analysis and Display System (GrADS) was used for plotting. This paper was partially supported by Universities Space Research Association.

1. Nuclear and Industrial Safety Agency (2011). Available at: <http://www.nisa.meti.go.jp/english/files/en20110321-1.pdf>. March 20, 2011.
2. Chino M, et al. (2011) Preliminary estimation of release amount of <sup>131</sup>I and <sup>137</sup>Cs accidentally discharged from the Fukushima Daiichi Nuclear Power Plant into the atmosphere. *J Nucl Sci Technol (Tokyo)* 48:1129–1134.
3. Hoetzlein RC (2011) Fukushima radiation—comparison map., Available at: <http://www.rchoetzlein.com/theory/2011/fukushima-radiation-comparison-map/>.
4. Unterwiesing MP, Hoppes DD, Schima FJ (1992) New and revised half-life measurements results. *Nucl Instrum Methods Phys Res Sect A* 312:349–352.
5. Filipovic-Vincekovic N, Barisic D, Masic N, Lulic S (1991) Distribution of fallout radionuclides through soil surface layer. *J Radioanal Nucl Chem* 148:53–62.
6. Giani L, Helmers H (1997) Migration of Cesium-137 in typical soils of North Germany ten years after the Chernobyl accident. *Z Pflanz Bodenkunde* 160:81–83.
7. Japanese Ministry of Education, Culture, Sports, Science, and Technology (MEXT) (2011) Readings of environmental radiation level of dust and soil by monitoring in schools in Fukushima Prefecture., Available at: <http://www.mext.go.jp/english/incident/1305657.htm>.
8. Morino Y, Ohara T, Nishizawa M (2011) Atmospheric behavior, deposition, and budget of radioactive materials from the Fukushima Daiichi nuclear power plant in March 2011. *Geophys Res Lett* L00G11.
9. Stohl A, Forster C, Frank A, Seibert P, Wotawa G (2005) The Lagrangian particle dispersion model FLEXPART version 6.2. *Atmos Chem Phys* 5:2461–2474.
10. Japanese Ministry of Education, Culture, Sports, Science, and Technology (MEXT) (2011) System for prediction of environment emergency dose information (SPEEDI)., Available at: [http://www.nsc.go.jp/mext\\_speedi/index.html](http://www.nsc.go.jp/mext_speedi/index.html) (in Japanese).
11. Japan Meteorological Agency (2011) Environmental Emergency Response., Available at: [http://www.jma.go.jp/jma/kokusai/eeer\\_list.html](http://www.jma.go.jp/jma/kokusai/eeer_list.html).
12. Takemura T, et al. (2011) A numerical simulation of global transport of atmospheric particles emitted from the Fukushima Daiichi Nuclear Power Plant. *SOLA* 7:101–104.
13. Visible Information Center Inc. (2011) Simulation on <sup>137</sup>Cs deposition due to the emission from Fukushima Daiichi Nuclear Plant., Available at: <http://www.vic.jp/fukushima/global/global-e.html>.
14. Japan Atomic Energy Agency (2011) A trial calculation on total amount of radiation exposure during 2 months after the accident of Fukushima Daiichi Nuclear Power Plant in TEPCO., Available at: <http://www.jaea.go.jp/jishin/kaisetsu03/kaisetsu03.htm> (in Japanese).
15. The EURAD project (2011) Potential dispersion of the radioactive cloud over the northern hemisphere., Available at: [http://www.eurad.uni-koeln.de/index\\_e.html](http://www.eurad.uni-koeln.de/index_e.html).
16. Deutscher Wetterdienst (2011) Deutscher Wetterdienst zu den Folgen der Fukushima-Katastrophe Wetter sorgt für starke Verdünnung der radioaktiven Konzentration., Available at: [http://www.dwd.de/bvbw/generator/DWDWWW/Content/Presse/Pressemittelungen/2011/20110323\\_Japan.templateId=raw,property=publicationFile.pdf/20110323\\_Japan.pdf](http://www.dwd.de/bvbw/generator/DWDWWW/Content/Presse/Pressemittelungen/2011/20110323_Japan.templateId=raw,property=publicationFile.pdf/20110323_Japan.pdf).
17. Japanese Ministry of Education, Culture, Sports, Science, and Technology (MEXT) (2011) Reading of radioactivity level in fallout by prefecture., Available at: <http://www.mext.go.jp/english/incident/1305529.htm>.
18. Japanese Ministry of Education, Culture, Sports, Science, and Technology (MEXT) (2011) Readings of sea area monitoring., Available at: <http://www.mext.go.jp/english/incident/1304192.htm>.
19. United Nations Scientific Committee on the Effects of Atomic Radiation (UNSCEAR) (2000) Sources and effects of ionizing radiation. *Sources Annex A*, Vol I (United Nations, New York), Available at: [http://www.unscear.org/unscear/en/publications/2000\\_1.html](http://www.unscear.org/unscear/en/publications/2000_1.html).
20. Japanese Ministry of Education, Culture, Sports, Science, and Technology (MEXT) (2011) Readings of environmental radioactivity level by prefecture., Available at: <http://www.mext.go.jp/english/incident/1304080.htm>.
21. Japanese Ministry of Education, Culture, Sports, Science, and Technology (MEXT) and the US Department of Energy (DOE) (2011) Results of Airborne Monitoring by the Ministry of Education, Culture, Sports, Science, and Technology and the US Department of Energy., Available at: <http://www.mext.go.jp/english/incident/1304796.htm>.
22. Japanese Ministry of Education, Culture, Sports, Science, and Technology (MEXT) (2011) Environmental radiation database., Available at: <http://search.kankyo-hoshano.go.jp/servlet/search.top>.
23. Tsukada H, Hisamatsu S, Inaba J (2003) Transfer of <sup>137</sup>Cs and stable Cs in soil-to-grass-milk pathway in Aomori., Japan. *J Radioanal Nucl Chem* 255:455–458.
24. Ministry of Agriculture, Forestry, and Fisheries (MAFF) (2011) A point of view on planting rice plant., Available at: [http://www.maff.go.jp/j/kanbo/joho/saigai/pdf/ine\\_sakutuke.pdf](http://www.maff.go.jp/j/kanbo/joho/saigai/pdf/ine_sakutuke.pdf) (in Japanese).
25. Holland DM (2000) Merged IBCAO/ETOPO5 global topographic data product. *National Geophysical Data Center (NGDC)*, Boulder Colorado, Available at: [http://efdl.cims.nyu.edu/project\\_aomip/forcing\\_data/topography/merged/overview.html](http://efdl.cims.nyu.edu/project_aomip/forcing_data/topography/merged/overview.html).
26. Japanese Ministry of Education, Culture, Sports, Science, and Technology (MEXT) (2011) Calculation results and basis regarding internal exposure studied in summarizing the tentative approach., Available at: [http://www.mext.go.jp/component/english/\\_icsFiles/afieldfile/2011/05/27/1306601\\_0512\\_1.pdf](http://www.mext.go.jp/component/english/_icsFiles/afieldfile/2011/05/27/1306601_0512_1.pdf).